$1/f$ noise in electrical conductors arising from the heterogeneous detrapping process of individual charge carriers

Aleksejus Kononovicius⋆ and Bronislovas Kaulakys

Institute of Theoretical Physics and Astronomy, Vilnius University,
Saulėtekio al. 3, 10257 Vilnius, Lithuania
⋆ aleksejus.kononovicius@tfai.vu.lt

October 11, 2023

Abstract

We propose a model of $1/f$ noise in electrical conductors based on the drift of individual charge carriers and their interaction with the trapping centers. We assume that the trapping centers are distributed uniformly across the material. The trapping centers are assumed to be heterogeneous and have unique detrapping rates, which are sampled from a uniform distribution. We show that under these assumptions, and if the trapping rate is low in comparison to the maximum detrapping rate, $1/f$ noise in the form of Hooge's relation is recovered. Hooge's parameter is shown to be a ratio between the characteristic trapping rate and the maximum detrapping rate.

Contents

---

1 Introduction

The nature of the $1/f$ noise (also referred to as flicker noise or pink noise), characterized by power spectral density of $S(f) \sim 1/f$ form, remains open to discussion despite almost 100 years since the first reports [1, 2]. While many materials, devices, and systems exhibit different kinds of fluctuations or noise [3–5], only the white noise and the Brownian noise are well understood starting from the first principles. White noise is characterized by absence of temporal correlations, and flat power spectral density of $S(f) \sim 1/f^0$ form. Examples of the white noise include thermal and shot noise. Thermal noise is known to arise from the random motion of the charge carriers. It occurs at any finite temperature regardless of whether the current flows. Shot noise, on the other hand, is a result of the discrete nature of the charge carriers and the Poisson statistics of waiting times before each individual detection of the charge carrier. The Brownian noise is a temporal integral of the white noise, and thus exhibits no correlations between the increments of the signal, it is characterized by a power spectral density of $S(f) \sim 1/f^2$ form.

Theory of $1/f$ noise based on the first principles is still an open problem. $1/f$ noise is of particular interest as it is observed across various physical [3, 4, 6–20], and non–physical [21–27] systems. As far as the $1/f$ noise cannot be obtained by the simple procedure of integration, differentiation, or simple transformation of some common signals, and the general mechanism generating such signals has not yet been identified, there is not generally accepted solution to this $1/f$ noise problem.

The oldest explanation for $1/f$ noise involves the superposition of Lorentzian spectra [28–33]. $1/f$ noise as a sum of the Lorentzian spectral densities also arises from the random telegraph signals [3], and from the Brownian motion with wide–range distribution of relaxations [34]. These approaches are often limited to the specific systems being modeled, or require quite restrictive assumptions to be satisfied [12, 13]. In the recent decades, series of models for the $1/f$ noise based on the specific, autoregressive AR(1), point process [34, 35], and the agent–based model [36, 37], yielding nonlinear stochastic differential equation [38] was proposed (see [39] for a recent review). Another more recent trend relies on scaling properties and non–linear transformations of signals [40–43]. These models, on the other hand, prove to be rather more abstract, and therefore more similar to the long–range memory models found in the mathematical literature, such as fractional Brownian motion [44–46] or ARCH models [47–50]. These and other similar models of $1/f$ noise are hardly applicable to the description and explanation of the mostly observable $1/f$ noise in the conductor materials.

On the other hand, for a homogeneous conductor material Hooge proposed an empirical relation for the $1/f$ noise dependence on the parameters of the material [51, 52],

$$S(f) = \bar{I}^2 \frac{\alpha_H}{N f}. \tag{1}$$

Where $\bar{I}$ stands for the average current flowing through the cross–section of the conductor material, N is the number of charge carriers, and α_H is the titular Hooge parameter. There were numerous attempts to derive or explain the structure of the Hooge's relation [3, 9, 10, 12, 33, 53–55]. In [35] Hooge's parameter was derived from an autoregressive point process model. More recent derivations of the Hooge's parameter based on the Poisson generation–recombination process modulated by the random telegraph noise were conducted in [56, 57]. These and similar models cannot be directly applied to describe and explain the widespread $1/f$ noise in the conductor materials.

Here, we propose a model of $1/f$ noise in electrical conductors containing heterogeneous trapping centers. As far as the square of the average current $\bar{I}^2$ is proportional to the squared number of charge carriers N^2, Hooge's relation implies that the intensity of $1/f$ noise is proportional to the number of charge carriers N. Therefore, as the first approximation we can consider the noise originating from the flow of individual charge carriers. It is known that the drift, and the diffusion, of the charge carries does not yield $1/f$ noise [3]. Therefore, we consider the drift of the charge carriers interrupted by their entrapment in the trapping centers. We show that, if the detrapping rates of individual trapping centers are heterogeneous and uniformly distributed, $1/f$ noise arises. In this model, the signal generated by a single charge carrier is similar to the signal from non–overlapping rectangular pulses [58]. Using the results of Ref. [58] we derive Hooge's relation, and show that Hooge's parameter is a ratio between the characteristic trapping rate and the maximum detrapping rate.

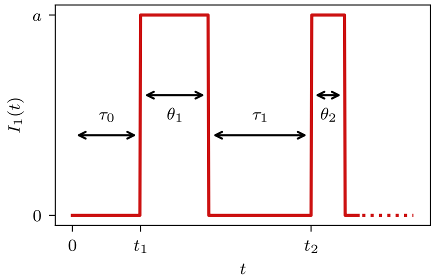

Figure 1: Current generated by a single charge carrier (red curve). Relevant notation: τ_i is the gap duration (detrapping time), θ_i is the pulse duration (trapping time), a is the height of the pulses (current generated by a single drifting charge carrier).

This paper is organized as follows. In Section 2 we introduce a general physical model for $1/f$ noise in the conductor materials based on the trapping–detrapping process of a single charge carrier. In Section 3 we discuss the implications of finite experiments and simulations. Namely, we show that the power spectral density produced by a single charge carrier may exhibit spurious low–frequency cutoff. This cutoff disappears, if the current generated by a large number of charge carriers is considered. Finally, Hooge's empirical relation and Hooge's parameter value for the proposed model is derived in Section 4. The main results are summarized in Section 5.

2 Model for $1/f$ noise in a homogeneous electrical conductor

Here we consider trapping–detrapping noise generated by a single charge carrier (e.g., electron). We consider only transitions between the conduction band and the trapping centers as producing fluctuations in the electric current. Under these conditions, the electric current generated by a single charge carrier is a sequence of non–overlapping rectangular pulses. The pulses are observed when the charge carrier drifts through the conduction band, thus generating the electric current. The pulses are separated by the gaps which correspond to the moments when the charge carrier remains trapped by any of the trapping centers. A sample signal generated by a single charge carrier is shown in Fig. 1.

In Fig. 1 and further in the paper τ_i will stand for i-th gap duration (detrapping time), θ_i will stand for i-th pulse duration (trapping time), and a will stand for the height of the pulses. The height of the pulses a has a fixed predetermined value as it represents the electric current generated by a drift of a single charge carrier. Gap and pulse durations are stochastic variables sampled from the specified gap and pulse duration distributions.

The power spectral density of a signal generated by a single charge carrier $I_1(t)$ (subscript 1 is added to emphasize that a single charge carrier is considered) composed of non–overlapping pulses with profiles $A_k(t)$ is given by

$$S_1(f) = \lim_{T\to\infty} \left\langle \frac{2}{T} \left| \int_0^T I_1(t) e^{-2\pi i f t} \, \mathrm{d}t \right|^2 \right\rangle = \\ = \lim_{T\to\infty} \left\langle \frac{2}{T} \left| \sum_k e^{-2\pi i f t_k} \mathcal{F}\{A_k(t-t_k)\} \right|^2 \right\rangle, \quad (2)$$

where T is the observation time, t_k is the start time of k-the pulse (corresponds to the time of k-th detrapping from the trapping center), and $\mathcal{F}\{A_k(t-t_k)\}$ stands for the Fourier transform of the k-th pulse profile $A_k(t-t_k)$. In the specific case considered here the pulse profiles differ only in their duration θ_k. If the pulse and gap durations are independent, then the power spectral density of the signal is determined purely by the height of the pulses a and the pulse and gap duration distributions (let $p_\theta(\theta)$ and $p_\tau(\tau)$ be their respective probability density functions). In this case, the general formula for the power spectral density is given by [58]

$$S_1(f)=\frac{a^2\bar{\nu}}{\pi^2 f^2}\mathrm{Re}\left[\frac{(1-\chi_\theta(f))(1-\chi_\tau(f))}{1-\chi_\theta(f)\chi_\tau(f)}\right]. \tag{3}$$

In the above

$$\chi_\tau(f)=\left\langle e^{2\pi i f\tau}\right\rangle=\int_0^\infty e^{2\pi i f\tau}p_\tau(\tau)\,\mathrm{d}\tau, \tag{4}$$

$$\chi_\theta(f)=\left\langle e^{2\pi i f\theta}\right\rangle=\int_0^\infty e^{2\pi i f\theta}p_\theta(\theta)\,\mathrm{d}\theta, \tag{5}$$

are the characteristic functions of the gap and pulse duration distributions respectively, and $\bar{\nu}$ is the mean number of pulses per unit time. For the ergodic processes, and given a long observation time, the value of $\bar{\nu}$ is trivially derived from the mean gap and mean burst durations, i.e., $\bar{\nu}=\frac{1}{\langle\theta\rangle+\langle\tau\rangle}$. For the nonergodic processes, or if the observation time is comparatively short, the value of $\bar{\nu}$ can be approximated by calculating the means from the truncated distributions, or it may be defined purely empirically, i.e., $\bar{\nu}=K/T$ (here K is the number of observed pulses, and T is the total observation time).

Typically when trapping–detrapping processes are considered [3, 11] it is assumed that both τ_i and θ_i are sampled from the exponential distributions with rates γ_τ and γ_θ respectively. Characteristic function of the exponential distribution, probability density function of which is given by

$$p(\tau)=\gamma\exp(-\gamma\tau), \tag{6}$$

with event rate γ, is given by

$$\chi(f)=\int_0^\infty \gamma e^{2\pi i f\tau-\gamma\tau}\,\mathrm{d}\tau=\frac{\gamma}{\gamma-2\pi i f}. \tag{7}$$

Inserting Eq. (7) as the characteristic function for pulse and gap duration distributions into Eq. (3) yields Lorentzian power spectral density [3]. Notably, there were prior works which have assumed that τ_i, θ_i, or both are sampled from the distributions with power–law tails [56–62]. Here, let us assume that the detrapping times in the individual trapping centers are sampled from an exponential distribution with a unique detrapping rate $\gamma_\tau^{(i)}$. This would correspond to the individual trapping centers having different potential depths or trapping to different quantum states of same trapping center. As well as a result of the redistribution through the states with small bounding energy as an outcome of the interaction with phonons, electrons, radiation, etc. If $\gamma_\tau^{(i)}$ is uniformly distributed in the interval from $\gamma_{\min}$ to $\gamma_{\max}$, then the probability density function of the detrapping time distribution is given by

$$\begin{aligned}p(\tau)&=\frac{1}{\gamma_{\max}-\gamma_{\min}}\int_{\gamma_{\min}}^{\gamma_{\max}}\gamma_\tau\exp(-\gamma_\tau\tau)\,\mathrm{d}\gamma_\tau=\\&=\frac{(1+\gamma_{\min}\tau)\exp(-\gamma_{\min}\tau)-(1+\gamma_{\max}\tau)\exp(-\gamma_{\max}\tau)}{(\gamma_{\max}-\gamma_{\min})\tau^2}.\end{aligned} \tag{8}$$

This probability density function saturates for the short detrapping times, $\tau\ll\frac{1}{\gamma_{\max}}$. For the longer detrapping times, $\tau\gg\frac{1}{\gamma_{\min}}$, it decays as an exponential function. In the intermediate

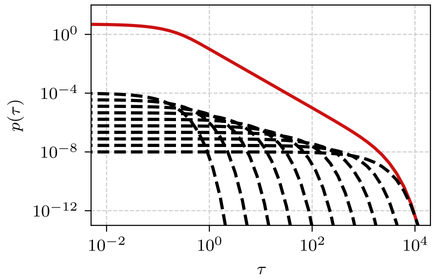

Figure 2: Probability density function of the detrapping time distribution under the assumption that detrapping rates of individual trapping centers are uniformly distributed (red curve), Eq. (8). The probability density function was calculated for $\gamma_{\text{min}} = 10^{-3}$, and $\gamma_{\text{max}} = 10$ case. Black dashed curves correspond to the exponential probability density functions of the detrapping times from the individual trapping centers with fixed rates: $\gamma_\tau = 10^{-3}$, 2.78×10^{-3}, 7.74×10^{-3}, 2.15×10^{-2}, 5.99×10^{-2}, 1.67×10^{-1}, 4.64×10^{-1}, 1.29, 3.59, and 10. Normalization of the exponential probability density functions was adjusted for the visualization purposes, but it remains proportional to their respective contributions.

value range, $\frac{1}{\gamma_{\text{max}}} \ll \tau \ll \frac{1}{\gamma_{\text{min}}}$, this probability density function has the τ^{-2} asymptotic behavior, which is already known to lead to $1/f$ noise [58–61]. The benefit of this formulation is that it allows to see how the τ^{-2} asymptotic behavior can emerge in homogeneous conductors. Experimentally τ^{-2} asymptotic behavior is observable in quantum dots, nanocrystal, nanorod, and other semiconductor materials [63–66], while the detrapping times can range from picoseconds to several months. The asymptotic behavior of Eq. (8) can be examined in Fig. 2 where it is represented by a red curve. Fig. 2 also highlights contributions of some of the individual trapping centers, detrapping time distributions of which are plotted as dashed black curves.

Unlike the simple power–law distribution, this gap duration distribution does not require the introduction of any arbitrary cutoffs. The parameters of this gap duration distribution have explicit physical meaning. Furthermore, the statistical moments are well–defined and have compact analytical forms. The mean of the distribution is given by

$$\langle \tau \rangle = \frac{1}{\gamma_{\text{max}} - \gamma_{\text{min}}} \ln\left(\frac{\gamma_{\text{max}}}{\gamma_{\text{min}}}\right), \tag{9}$$

while the higher order moments are given by

$$\langle \tau^q \rangle = \frac{q!}{\gamma_{\text{max}} - \gamma_{\text{min}}} \times \frac{\gamma_{\text{min}}^{1-q} - \gamma_{\text{max}}^{1-q}}{q-1}. \tag{10}$$

The characteristic function of the gap duration distribution can be obtained either by inserting Eq. (8) into Eq. (4), or by averaging over the characteristic functions of the exponential distribution, Eq. (7). Latter approach yields the expression quicker

$$\chi_\tau(f) = \frac{1}{\gamma_{\text{max}} - \gamma_{\text{min}}} \int_{\gamma_{\text{min}}}^{\gamma_{\text{max}}} \frac{\gamma_\tau}{\gamma_\tau - 2\pi\mathrm{i}f}\, \mathrm{d}\gamma_\tau = 1 + \frac{2\pi\mathrm{i}f}{\gamma_{\text{max}} - \gamma_{\text{min}}} \ln\left(\frac{\gamma_{\text{max}} - 2\pi\mathrm{i}f}{\gamma_{\text{min}} - 2\pi\mathrm{i}f}\right). \tag{11}$$

If the interval of the possible detrapping rates is broad $\gamma_{\text{min}} \ll \gamma_{\text{max}}$, then for $\gamma_{\text{min}} \ll 2\pi f \ll \gamma_{\text{max}}$ the characteristic function can be approximated by

$$\chi_\tau(f) \approx 1 + \frac{2\pi\mathrm{i}f}{\gamma_{\text{max}}} \ln\left(1 + \frac{\mathrm{i}\gamma_{\text{max}}}{2\pi f}\right) \approx 1 - \frac{2\pi f}{\gamma_{\text{max}}}\left[\frac{\pi}{2} - \mathrm{i}\ln\left(\frac{2\pi f}{\gamma_{\text{max}}}\right)\right]. \tag{12}$$

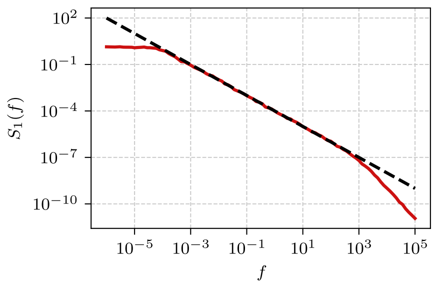

Figure 3: Power spectral density of the simulated signal (red curve) and its analytical approximation by Eq. (14) (black dashed curve). Simulated power spectral density was obtained by averaging over 10^2 realizations. Simulation parameters: $T = 10^6$, $\gamma_{\min} = 10^{-4}$, $\gamma_{\max} = 10^4$, $a = 1$, $\gamma_\theta = 1$.

Inserting Eq. (12) into Eq. (3) we have

$$S_1(f) = \frac{2a^2\bar{\nu}}{\pi\gamma_{\max}f}\,\mathrm{Re}\left[\frac{(1-\chi_\theta(f))\left[\frac{\pi}{2} - \mathrm{i}\ln\left(\frac{2\pi f}{\gamma_{\max}}\right)\right]}{1-\chi_\theta(f)\left\{1-\frac{2\pi f}{\gamma_{\max}}\left[\frac{\pi}{2} - \mathrm{i}\ln\left(\frac{2\pi f}{\gamma_{\max}}\right)\right]\right\}}\right]. \tag{13}$$

Assuming that $\frac{2\pi f}{\gamma_{\max}}\left[\frac{\pi}{2} - \mathrm{i}\ln\left(\frac{2\pi f}{\gamma_{\max}}\right)\right] \ll 1$, which is supported by an earlier assumption that $2\pi f \ll \gamma_{\max}$, allows to simplify the above to

$$S_1(f) \approx \frac{a^2\bar{\nu}}{\gamma_{\max}f}. \tag{14}$$

This approximation should hold well for $\gamma_{\min} \ll 2\pi f \ll \gamma_{\max}$, and should not depend on the explicit form of $\chi_\theta(f)$ unless $\chi_\theta(f) \approx 1$ for at least some of the frequencies in the range.

Let us examine a specific case when the trapping centers are uniformly distributed within the material, and therefore the trapping process can be assumed to be a homogeneous Poisson process. Inserting the characteristic function of the exponential distribution, Eq. (7), as the characteristic function of the pulse duration distribution into Eq. (3) yields

$$S_1(f) = \frac{4a^2\bar{\nu}}{\gamma_\theta^2}\,\mathrm{Re}\left[\frac{1}{1-\chi_\tau(f) - \frac{2\pi \mathrm{i} f}{\gamma_\theta}}\right]. \tag{15}$$

Then inserting the characteristic function of the proposed detrapping time distribution, Eq. (12), into Eq. (15) yields

$$S_1(f) = \frac{a^2\bar{\nu}\gamma_{\max}}{\gamma_\theta^2 f} \times \frac{1}{\left(\frac{\pi}{2}\right)^2 + \left[\frac{\gamma_{\max}}{\gamma_\theta} + \ln\left(\frac{2\pi f}{\gamma_{\max}}\right)\right]^2}. \tag{16}$$

If the maximum detrapping rate is large in comparison to the trapping rate, i.e. $\frac{\gamma_{\max}}{\gamma_\theta} \gg \frac{\pi}{2}$ and $\frac{\gamma_{\max}}{\gamma_\theta} \gg -\ln\left(\frac{2\pi f}{\gamma_{\max}}\right)$, then we recover Eq. (14). In Fig. 3 the power spectral density of a simulated signal with comparatively large detrapping rates is shown as a red curve.

3 Low–frequency cutoff in finite experiments

The obtained approximation, Eq. (14), holds in the infinite observation time limit (single infinitely long signal) or the infinite number of experiments limit (infinitely many signals with finitely long observation time). If either of the limits doesn't hold, then the range of frequencies over which the pure $1/f$ noise is observed becomes narrower. In the finite experiments the process will not reach a steady state, and therefore the cutoff frequencies will depend not on the model parameter values γ_{min} and γ_{max}, but on the smallest and the largest $\gamma_\tau^{(i)}$ values actually observed during the experiment. The difference between γ_{max} and the largest $\gamma_\tau^{(i)}$ is negligible, because the pure $1/f$ noise will be observed only if γ_{max} is a relatively large number. On the other hand the relative difference between γ_{min} and smallest $\gamma_\tau^{(i)}$ might not be negligible. Let us estimate the expected value of the smallest $\gamma_\tau^{(i)}$ in a finite experiment.

In the model introduced in the previous section $\gamma_\tau^{(i)}$ is sampled from the uniform distribution with $[\gamma_{\mathrm{min}}, \gamma_{\mathrm{max}}]$ range of possible values. It is known that, for x_i sampled from the uniform distribution with $[0,1]$ range of possible values, the smallest x_i observed in the sample of size K is distributed according to the Beta distribution with the shape parameters $\alpha = 1$ and $\beta = K$ [67]. Thus the expected value of the smallest x_i is given by

$$\left\langle \min\{x_i\}_K \right\rangle = \frac{\alpha}{\alpha+\beta} = \frac{1}{K+1}. \tag{17}$$

Rescaling the range of possible values to $[\gamma_{\mathrm{min}}, \gamma_{\mathrm{max}}]$ yields

$$\gamma_{\mathrm{min}}^{(\mathrm{eff})} = \left\langle \min\{\gamma_\tau^{(i)}\}_K \right\rangle = \frac{\gamma_{\mathrm{max}} - \gamma_{\mathrm{min}}}{K+1} + \gamma_{\mathrm{min}}. \tag{18}$$

As K corresponds to the number of pulses in the signal, we have that $K = \bar{\nu} T = \frac{T}{\langle\theta\rangle + \langle\tau\rangle}$ and

$$\gamma_{\mathrm{min}}^{(\mathrm{eff})} = (\gamma_{\mathrm{max}} - \gamma_{\mathrm{min}}) \frac{\langle\theta\rangle + \langle\tau\rangle}{\langle\theta\rangle + \langle\tau\rangle + T} + \gamma_{\mathrm{min}}. \tag{19}$$

In the above $\langle\theta\rangle$ is effectively a model parameter as it is trivially given by $\langle\theta\rangle = \frac{1}{\gamma_\theta}$, while $\langle\tau\rangle$ is a derived quantity which has a more complicated dependence on the model parameters γ_{min} and γ_{max} (see Eq. (9)). If the range of possible $\gamma_\tau^{(i)}$ values is broad, i.e., $\gamma_{\mathrm{max}} \gg \gamma_{\mathrm{min}}$, we have

$$\gamma_{\mathrm{min}}^{(\mathrm{eff})} \approx \gamma_{\mathrm{max}} \frac{\gamma_{\mathrm{max}} \langle\theta\rangle + \ln\frac{\gamma_{\mathrm{max}}}{\gamma_{\mathrm{min}}}}{\gamma_{\mathrm{max}}(\langle\theta\rangle + T) + \ln\frac{\gamma_{\mathrm{max}}}{\gamma_{\mathrm{min}}}} + \gamma_{\mathrm{min}}. \tag{20}$$

The above applies to the ergodic case with $\gamma_{\mathrm{min}} \gg 1/T$. In the nonergodic case, for $\gamma_{\mathrm{min}} \lesssim 1/T$, it would impossible to distinguish between the cases corresponding to the different γ_{min} values. Therefore, for the nonergodic case, γ_{min} can be replaced by $1/T$ yielding

$$\gamma_{\mathrm{min}}^{(\mathrm{eff})} \approx \gamma_{\mathrm{max}} \frac{\gamma_{\mathrm{max}} \langle\theta\rangle + \ln(\gamma_{\mathrm{max}} T)}{\gamma_{\mathrm{max}}(\langle\theta\rangle + T) + \ln(\gamma_{\mathrm{max}} T)} + \frac{1}{T} \approx \frac{1 + \gamma_{\mathrm{max}} \langle\theta\rangle + \ln(\gamma_{\mathrm{max}} T)}{T}. \tag{21}$$

For relatively long pulse durations, $\langle\theta\rangle \gg \frac{\ln(\gamma_{\mathrm{max}} T)}{\gamma_{\mathrm{max}}}$, we have that

$$\gamma_{\mathrm{min}}^{(\mathrm{eff})} \approx \frac{1 + \gamma_{\mathrm{max}} \langle\theta\rangle}{T} \approx \frac{\gamma_{\mathrm{max}}}{\gamma_\theta T}. \tag{22}$$

From the above, it follows that low–frequency cutoff is always present in singular experiments with one charge carrier, and with finite observation time T. The cutoff will be observed at a frequency close to $\gamma_{\mathrm{min}}^{(\mathrm{eff})}$. As can be seen in Fig. 4, the cutoff moves to the lower frequencies as T increases, the power spectral density is flat for the lowest observable natural frequencies, $\frac{1}{T} < f \lesssim \frac{\gamma_{\mathrm{max}}}{\gamma_\theta T}$.

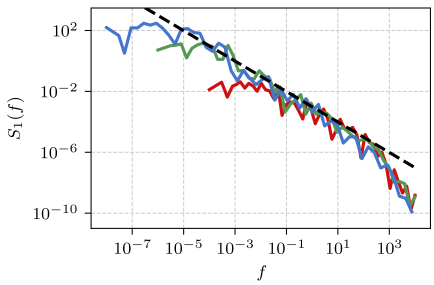

Figure 4: The effect of increasing the observation time on the obtained power spectral density. Dashed black curve corresponds to Eq. (14). Simulation parameters: $a = 1$, $\gamma_\theta = 1$, $\gamma_{\min} = 0$, $\gamma_{\max} = 10^3$, $T = 10^4$ (red curve), 10^6 (green curve), and 10^8 (blue curve).

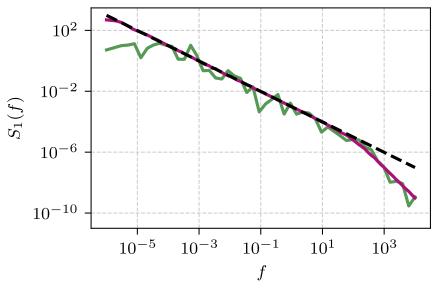

Figure 5: The effect of averaging over repeated experiments on the obtained power spectral density: $R = 1$ (green curve), $R = 10^3$ (magenta curve). Dashed black curve corresponds to Eq. (14). Simulation parameters, with exception to R, are the same as for the green curve from Fig. 4.

If multiple independent experiments (let R be the number of experiments) with finite observation time T are performed and the obtained spectral densities are averaged, then the total number of observed pulses increases by a factor of R yielding

$$\gamma_{\min}^{(\mathrm{eff})} = (\gamma_{\max} - \gamma_{\min}) \frac{\langle\theta\rangle + \langle\tau\rangle}{\langle\theta\rangle + \langle\tau\rangle + RT} + \gamma_{\min} \approx \frac{\gamma_{\max}\langle\theta\rangle}{RT} + \frac{1}{T} = \frac{R + \gamma_{\max}\langle\theta\rangle}{RT}. \tag{23}$$

For $R \gg \gamma_{\max}\langle\theta\rangle$, no low–frequency cutoff will be noticeable. As shown in Fig. 5, low–frequency cutoff disappears as the experiments are repeated and the obtained power spectral densities are averaged.

We have derived Eq. (14) considering the current generated by a single charge carrier. In many experiments the number of charge carriers N will be large, $N \gg 1$. Consequently, from the Wiener–Khinchin theorem [3] it follows that performing independent experiments is equivalent to observing independent charge carriers. Therefore for $N \gg \gamma_{\max}\langle\theta\rangle$ no low–frequency cutoff will be noticeable. Though in this case, the power spectral densities of the signals generated by single charge carriers add up instead of averaging out, yielding a minor generalization of Eq. (14)

$$S_N(f) \approx \frac{N a^2 \bar{\nu}}{\gamma_{\max} f}. \tag{24}$$

In the above $\bar{\nu}$ is strictly the mean number of pulses per unit time generated by a single charge carrier.

As can be seen in Fig. 6 (a), the signal generated by multiple independent charge carriers is no longer composed of non–overlapping pulses, although it retains discrete nature as

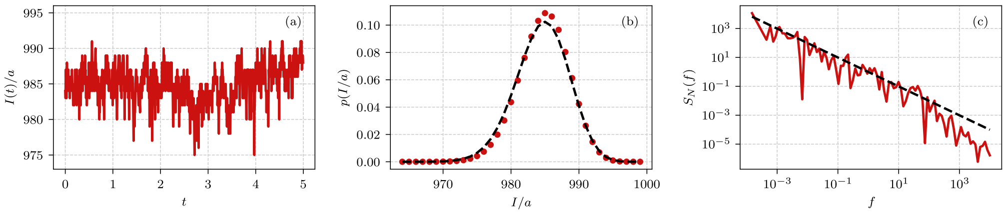

Figure 6: Sample of a signal generated by 10^3 independent charge carriers (a), the probability mass function of the amplitude of the signal (b), and the power spectral density of the signal (c). Red curves represent results of numerical simulation, while dashed black curves provide theoretical fits: (b) Binomial probability mass function with $p_F \approx 0.984$ and $N = 10^3$, (c) the power spectral density approximation Eq. (24). Simulation parameters: $R = 1$, $N = 10^3$, $T = 6710.8864$, $a = 1$, $\gamma_\theta = 1$, $\gamma_{\min} = 0$, $\gamma_{\max} = 10^3$.

individual charges drift freely or are trapped by the trapping centers. The amplitude and the slope of the power spectral density are well predicted by Eq. (24) (as seen in Fig. 6 (c)). The distribution of the signal's amplitude would be expected to follow the Binomial distribution with sample size N and success probability (probability that the charge carrier is free)

$$p_F = \frac{\langle\theta\rangle}{\langle\theta\rangle + \langle\tau\rangle} \approx 1 - \frac{\langle\tau\rangle}{\langle\theta\rangle}. \tag{25}$$

The fit by the Binomial distribution shown in Fig. 6 (b) is not perfect, because the nonergodic case is simulated and $\langle\tau\rangle$ is ill–defined, but predicts the overall shape of the probability distribution rather well. For $\gamma_{\min} \gg 1/T$ the fit would be much better. Notably, with larger N and under noisy observation, the Binomial distribution predicted by the model will quickly become indistinguishable from the Gaussian distribution. While in some cases $1/f$ noise is known to behave as a non–Gaussian process, most often it is found to exhibit Gaussian fluctuations [3, 68, 69].

Notably, [70] also discusses a spurious low–frequency cutoff that could be observed in single particle experiments. Of the $1/f$ noise models considered in [70] superimposed random telegraph signals and blinking quantum dot models are the most comparable to the model presented here. In [70] each of the superimposed random telegraph signals was assumed to be characterized by their own Poissonian switching rate $\gamma = \gamma_\theta = \gamma_\tau$ between the "on" and "off" states. It was shown that the conditional power spectral density (requiring a certain minimum number of pulses, $K_{\min}$, to be observed) exhibits low–frequency cutoff at $f_c \sim K_{\min}/T$. In our simulations, we typically observe a large number of pulses, $K \approx \gamma_\theta T$, and should therefore observe the cutoff at $f_c \sim \gamma_\theta$, but instead, we observe that the cutoff frequency scales as $1/\gamma_\theta$. The nature of the cutoff is different in the model introduced here. The other, blinking quantum dot, model does not predict low–frequency cutoff, only the ageing effect, which for the pure $1/f$ noise will not be noticeable [58].

4 Derivation of Hooge's empirical relation and Hooge's parameter

It is straightforward to see that we can rewrite Eq. (24) in the form of Hooge's empirical relation, Eq. (1), if we define Hooge's parameter as

$$\alpha_H = \frac{N^2 a^2 \bar{\nu}}{\gamma_{\max} \bar{I}^2}. \tag{26}$$

Further we show that the straightforward expression above can be simplified, and given a more compact form.

As the height of the pulses a corresponds to the current generated by a single charge carrier we have

$$a = \frac{q v_c}{L}, \tag{27}$$

where q stands for the charge held by the carrier, v_c is the drift velocity between the trappings, and L is the length of the material. Expression for a can be rewritten in terms of the average current flowing through the cross–section of the material σ_M

$$\bar{I} = \sigma_M n q v_d, \tag{28}$$

where n stands for the density of the charge carriers (i.e., $n = \frac{N}{L\sigma_M}$), and v_d is the average velocity of the charge carriers. The average velocity is related to the free drift velocity via the fraction of time the charge carrier spends drifting

$$v_d = \frac{\langle\theta\rangle}{\langle\theta\rangle + \langle\tau\rangle} v_c = \bar{\nu}\langle\theta\rangle v_c. \tag{29}$$

Consequently we have

$$a = \frac{\bar{I}}{N\bar{\nu}\langle\theta\rangle}. \tag{30}$$

Inserting Eq. (30) into Eq. (26) yields the expression of the Hooge's parameter in terms of the characteristic trapping rate and the maximum detrapping rate, assuming that the pulses are comparatively long $\langle\theta\rangle \gg \langle\tau\rangle$,

$$\alpha_H = \frac{1}{\bar{\nu}\langle\theta\rangle^2 \gamma_{\max}} \approx \frac{\gamma_\theta}{\gamma_{\max}} = \frac{\langle\tau_{\min}\rangle}{\langle\theta\rangle}. \tag{31}$$

In the above $\langle\tau_{\min}\rangle = \frac{1}{\gamma_{\max}}$ is the expected gap duration generated when a charge carrier is trapped by the shallowest trapping center. The purer materials (i.e., ones with lower trapping center density n_c) will have lower α_H values, as the trapping rate is given by $\gamma_\theta = \langle\sigma_c v_c\rangle n_c$ (here σ_c is the trapping cross–section).

Consequently the approximations for the power spectral density generated by the proposed model, Eqs. (14) and (24), can be rewritten in the same form as Hooge's empirical relation. Inserting Eq. (31) into Eq. (1) yields

$$S_N(f) = \bar{I}^2 \frac{\gamma_\theta}{\gamma_{\max} N f}. \tag{32}$$

This expression appears to imply that the process under consideration is stationary, but this is not true as the average current $\bar{I}$ is proportional to the number of pulses per unit time $\bar{\nu}$, which in the $\gamma_{\min} \to 0$ limit is a function of the observation time T [58]. Although, for the case of pure $1/f$ noise, the dependence on T is logarithmically slow, and barely noticeable. Nevertheless, even if the process would be non–stationary, this should not have any impact on the estimate of Hooge's parameter as only $\bar{I}$ is impacted by the non–stationarity.

5 Conclusions

We have proposed a general physical model of $1/f$ noise based on the trapping–detrapping process in homogeneous electrical conductors. Unlike in the previous works, we have assumed that the detrapping rate of each trapping center is random, and sampled from the uniform distribution. This assumption leads to a power–law distribution of the detrapping times Eq. (8), which arises from a superposition of exponential detrapping time distributions representing the individual trapping centers with their own detrapping rates (see Fig. 2). Under this assumption, regardless of the details of the trapping process, as long as the trapping process is slow in comparison to the detrapping process, pure $1/f$ noise in a form of Hooge's empirical relation is obtained, Eq. (32). Under the assumptions of the proposed model, Hooge's parameter is just a ratio between the rate parameters of the trapping and the detrapping processes Eq. (31).

In Section 3, we have noted that as long as a finite signal generated by a single charge carrier is considered, the power spectral density may exhibit spurious low–frequency cutoff. The cutoff width is of the same order of magnitude as $\frac{\gamma_{\max}}{\gamma_\theta}$. This cutoff disappears when the power spectral density is averaged over a large number of experiments of finitely long observation time, or when the power spectral density is generated by a large number of independent charge carriers over finitely long observation time. In the latter case the distribution of the signal's amplitude follows Binomial distribution, which under noisy observations will quickly become indistinguishable from the Gaussian distribution.

Future extensions of the approach presented here could include a more detailed analysis of multiple charge carrier dynamics, and allowing the detrapping rates to come from a discrete uniform distribution with a reasonably small number of possible detrapping rate values.

All of the code used to perform the reported numerical simulations is available in [71].

Author contributions Conceptualization (BK), Software (AK), Validation (AK), Visualization (AK), Writing (AK, BK).

References

[1] J. B. Johnson, *The Schottky effect in low frequency circuits*, Physical Review **26**, 71 (1925), doi:10.1103/PhysRev.26.71.

[2] W. Schottky, *Small-shot effect and flicker effect*, Physical Review **28**(1), 74 (1926), doi:10.1103/PhysRev.28.74.

[3] S. Kogan, *Electronic noise and fluctuations in solids*, Cambridge University Press, doi:10.1017/CBO9780511551666 (1996).

[4] S. B. Lowen and M. C. Teich, *Fractal-Based Point Processes*, Wiley, doi:10.1002/0471754722 (2005).

[5] N. G. van Kampen, *Stochastic process in physics and chemistry*, North Holland, Amsterdam (2007).

[6] R. F. Voss and J. Clarke, *1/f noise from systems in thermal qquilibrium*, Physical Review Letters **36**(1), 42 (1976), doi:10.1103/PhysRevLett.36.42.

[7] P. Dutta and P. M. Horn, *Low-frequency fluctuations in solids: 1/f noise*, Reviews of Modern Physics **53**, 497 (1981), doi:10.1103/RevModPhys.53.497.

[8] M. B. Weissman, *1/f noise and other slow, nonexponential kinetics in condensed matter*, Reviews of Modern Physics **60**(2), 537 (1988), doi:10.1103/RevModPhys.60.537.

[9] F. N. Hooge, T. G. M. Kleinpenning and L. K. J. Vandamme, *Experimental studies on 1/f noise*, Reports on Progress in Physics **44**(5), 479 (1981), doi:10.1088/0034-4885/44/5/001.

[10] F. N. Hooge, *1/f noise sources*, IEEE Transactions on Electron Devices **41**(11), 1926 (1994), doi:10.1109/16.333808.

[11] V. Mitin, L. Reggiani and L. Varani, *Generation-recombination noise in semiconductors*, In *Noise and Fluctuation Controls in Electronic Devices*, Noise and Fluctuation Controls in Electronic Devices. American Scientific Publishers (2002).

[12] H. Wong, *Low-frequency noise study in electron devices: Review and update*, Microelectronics Reliability **43**(4), 585 (2003), doi:10.1016/S0026-2714(02)00347-5.

[13] D. M. Fleetwood, *1/f noise and defects in microelectronic materials and devices*, IEEE Transactions on Nuclear Science **62**(4), 1462 (2015), doi:10.1109/tns.2015.2405852.

[14] G. Careri and G. Consolini, *Dielectric 1/f noise of proton glass on a hydrated protein surface*, Physical Review E **62**(3), 4454 (2000), doi:10.1103/PhysRevE.62.4454.

[15] Z. Siwy and A. Fuliński, *Origin of 1/f noise in membrane channel currents*, Physical Review Letters **89**(15), 158101 (2002), doi:10.1103/PhysRevLett.89.158101.

[16] A. A. Balandin, *Low-frequency 1/f noise in graphene devices*, Nature Nanotechnology **8**, 549 (2013), doi:10.1038/nnano.2013.144.

[17] J.-O. Krisponeit, C. Kalkert, B. Damaschke, V. Moshnyaga and K. Samwer, *Time-resolved resistive switching on manganite surfaces: Creep and $1/f^{\alpha}$ noise signatures indicate pinning of nanoscale domains*, Physical Review B **87**(12), 121103(R) (2013), doi:10.1103/PhysRevB.87.121103.

[18] S. Sadegh, E. Barkai and D. Krapf, *1/f noise for intermittent quantum dots exhibits non-stationarity and critical exponents*, New Journal of Physics **16**, 113054 (2014), doi:10.1088/1367-2630/16/11/113054.

[19] Z. R. Fox, E. Barkai and D. Krapf, *Aging power spectrum of membrane protein transport and other subordinated random walks*, Nature Communications **12** (2021), doi:10.1038/s41467-021-26465-8.

[20] G. Wirth, M. B. da Silva and T. H. Both, *Unified compact modeling of charge trapping in 1/f noise, RTN and BTI*, In *2021 5th IEEE Electron Devices Technology and Manufacturing Conference (EDTM)*, pp. 1–3. IEEE, doi:10.1109/edtm50988.2021.9421005 (2021).

[21] R. F. Voss and J. Clarke, *1/f noise in music and speech*, Nature **258**, 317 (1975), doi:10.1038/258317a0.

[22] M. Kobayashi and T. Musha, *1/f fluctuation of heartbeat period*, IEEE Transactions on Biomedical Engineering **29**, 456 (1982), doi:10.1109/TBME.1982.324972.

[23] D. L. Gilden, T. Thornton and M. W. Mallon, *$1/f$ noise in human cognition*, Science **267**(5205), 1837 (1995), doi:10.1126/science.7892611.

[24] E.-J. Wagenmakers, S. Farrell and R. Ratcliff, *Estimation and interpretation of $1/f^{\alpha}$ noise in human cognition*, Psychonomic Bulletin & Review **11**, 579 (2004), doi:10.3758/bf03196615.

[25] W. Li and D. Holste, *Universal 1/f noise, crossovers of scaling exponents, and chromosome-specific patterns of guanine-cytosine content in DNA sequences of the human genome*, Physical Review E **71**(4), 041910 (2005), doi:10.1103/PhysRevE.71.041910.

[26] B. Podobnik, D. Horvatic, A. L. Ng, H. E. Stanley and P. C. Ivanov, *Modeling long-range cross-correlations in two-component ARFIMA and FIARCH processes*, Physica A **387**(15), 3954 (2008), doi:10.1016/j.physa.2008.01.062.

[27] D. J. Levitin, P. Chordia and V. Menon, *Musical rhythm spectra from Bach to Joplin obey a 1/f power law*, Proceedings of the National Academy of Sciences of the United States of America **109**, 3716 (2012), doi:10.1073/pnas.1113828109.

[28] J. Bernamont, *Fluctuations in the resistance of thin films*, Proceedings of the Physical Society **49**(4S), 138 (1937), doi:10.1088/0959-5309/49/4S/316.

[29] M. Surdin, *Fluctuations de courant thermionique et le Flicker effect*, Journal de Physique et le Radium **10**(4), 188 (1939), doi:10.1051/jphysrad:01939001004018800.

[30] M. Surdin, *Une théorie des fluctuations électriques dans les semi-conducteurs*, Journal de Physique et le Radium **12**(8), 777 (1951), doi:10.1051/jphysrad:01951001208077700.

[31] A. L. McWhorter and R. H. Kingston, *Semiconductor surface physics*, In *Proceedings of the Conference on Physics of Semiconductor Surface Physics*, vol. 207. University of Pennsylvania, Philadelphia (1957).

[32] A. V. D. Ziel, *Flicker noise in electronic devices*, In *Advances in Electronics and Electron Physics*, pp. 225–297. Elsevier, doi:10.1016/s0065-2539(08)60768-4 (1979).

[33] V. Palenskis and K. Maknys, *Nature of low-frequency noise in homogeneous semiconductors*, Scientific Reports **5**(1) (2015), doi:10.1038/srep18305.

[34] B. Kaulakys, V. Gontis and M. Alaburda, *Point process model of 1/f noise vs a sum of Lorentzians*, Physical Review E **71**, 051105 (2005), doi:10.1103/PhysRevE.71.051105.

[35] B. Kaulakys, *Autoregressive model of 1/f noise*, Physics Letters A **257**, 37 (1999), doi:10.1016/S0375-9601(99)00284-4.

[36] J. Ruseckas, B. Kaulakys and V. Gontis, *Herding model and 1/f noise*, EPL **96**, 60007 (2011), doi:10.1209/0295-5075/96/60007.

[37] A. Kononovicius and V. Gontis, *Agent based reasoning for the non-linear stochastic models of long-range memory*, Physica A **391**, 1309 (2012), doi:10.1016/j.physa.2011.08.061.

[38] B. Kaulakys and M. Alaburda, *Modeling scaled processes and $1/f^{\beta}$ noise using non-linear stochastic differential equations*, Journal of Statistical Mechanics **2009**(02), P02051 (2009), doi:10.1088/1742-5468/2009/02/p02051.

[39] R. Kazakevicius, A. Kononovicius, B. Kaulakys and V. Gontis, *Understanding the nature of the long–range memory phenomenon in socioeconomic systems*, Entropy **23**, 1125 (2021), doi:10.3390/e23091125.

[40] J. Ruseckas and B. Kaulakys, *Scaling properties of signals as origin of 1/f noise*, Journal of Statistical Mechanics **2014**(6), P06005 (2014), doi:10.1088/1742-5468/2014/06/p06005.

[41] B. Kaulakys, M. Alaburda and J. Ruseckas, *1/f noise from the nonlinear transformations of the variables*, Modern Physics Letters B **29**, 1550223 (2015), doi:10.1142/S0217984915502231.

[42] I. Eliazar, *Selfsimilar diffusions*, Journal of Physics A: Mathematical and Theoretical **54**, 35LT01 (2021), doi:10.1088/1751-8121/ac1771.

[43] R. Kazakevičius and A. Kononovicius, *Anomalous diffusion and long-range memory in the scaled voter model*, Physical Review E **107**, 024106 (2023), doi:10.1103/PhysRevE.107.024106.

[44] B. Mandelbrot and J. W. Van Ness, *Fractional Brownian motions, fractional noises and applications*, SIAM Review **10**, 422 (1968), doi:10.1137/1010093.

[45] B. B. Mandelbrot, *Multifractals and 1/f noise: Wild self-affinity in physics (1963–1976)*, Springer (2013).

[46] J. Beran, *Statistics for long-memory processes*, Routledge, doi:10.1201/9780203738481 (2017).

[47] R. Engle, *Autoregresive conditional heteroscedasticity with estimates of the variance of United Kingdom inflation*, Econometrica **50**, 987 (1982), doi:10.2307/1912773.

[48] T. Bollerslev, *Generalized autoregressive conditional heteroskedasticity*, Journal of Econometrics **31**, 307 (1986), doi:10.1016/0304-4076(86)90063-1.

[49] L. Giraitis, R. Leipus and D. Surgailis, *ARCH(∞) models and long memory*, In T. G. Anderson, R. A. Davis, J. Kreis and T. Mikosh, eds., *Handbook of Financial Time Series*, pp. 71–84. Springer Verlag, Berlin, doi:10.1007/978-3-540-71297-8_3 (2009).

[50] T. Bollerslev, *The story of GARCH: A personal odyssey*, Journal of Econometrics **234**, 96 (2023), doi:10.1016/j.jeconom.2023.01.015.

[51] F. N. Hooge, *1/f noise is no surface effect*, Physics Letters A **29**(3), 139 (1969), doi:10.1016/0375-9601(69)90076-0.

[52] F. N. Hooge, *Discussion of recent experiments on 1/f noise*, Physica **60**(1), 130 (1972), doi:10.1016/0031-8914(72)90226-1.

[53] F. Hooge, *The relation between 1/f noise and number of electrons*, Physica B: Condensed Matter **162**(3), 344 (1990), doi:10.1016/0921-4526(90)90030-X.

[54] A. P. Dmitriev, M. E. Levinshtein and S. L. Rumyantsev, *On the hooge relation in semiconductors and metals*, Journal of Applied Physics **106**(2), 024514 (2009), doi:10.1063/1.3186620.

[55] L. K. J. Vandamme, *How useful is Hooge's empirical relation*, In *22nd International Conference on Noise and Fluctuations (ICNF)*, pp. 1–6. IEEE, doi:10.1109/ICNF.2013.6578875 (2013).

[56] F. Gruneis, *An alternative form of Hooge's relation for 1/f noise in semiconductor materials*, Physics Letters A **383**(13), 1401 (2019), doi:10.1016/j.physleta.2019.02.009.

[57] F. Gruneis, *1/f noise under drift and thermal agitation in semiconductor materials*, Physica A **593**, 126917 (2022), doi:10.1016/j.physa.2022.126917.

[58] A. Kononovicius and B. Kaulakys, *1/f noise from the sequence of nonoverlapping rectangular pulses*, Physical Review E **107**, 034117 (2023), doi:10.1103/PhysRevE.107.034117.

[59] G. Margolin and E. Barkai, *Nonergodicity of a time series obeying Levy statistics*, Journal of Statistical Physics **122**(1), 137 (2006), doi:10.1007/s10955-005-8076-9.

[60] M. Lukovic and P. Grigolini, *Power spectra for both interrupted and perennial aging processes*, The Journal of Chemical Physics **129**(18), 184102 (2008), doi:10.1063/1.3006051.

[61] M. Niemann, H. Kantz and E. Barkai, *Fluctuations of 1/f noise and the low-frequency cutoff paradox*, Physical Review Letters **110**(14), 140603 (2013), doi:10.1103/PhysRevLett.110.140603.

[62] N. Leibovich, A. Dechant, E. Lutz and E. Barkai, *Aging Wiener-Khinchin theorem and critical exponents of $1/f^{\beta}$ noise*, Physical Review E **94**, 052130 (2016), doi:10.1103/PhysRevE.94.052130.

[63] P. Frantsuzov, M. Kuno, B. Jankó and R. A. Marcus, *Universal emission intermittency in quantum dots, nanorods and nanowires*, Nature Physics **4**(7), 519 (2008), doi:10.1038/nphys1001.

[64] A. A. Cordones and S. R. Leone, *Mechanisms for charge trapping in single semiconductor nanocrystals probed by fluorescence blinking*, Chemical Society Reviews **42**(8), 3209 (2013), doi:10.1039/c2cs35452g.

[65] A. V. Nenashev, V. V. Valkovskii, J. O. Oelerich, A. V. Dvurechenskii, O. Semeniuk, A. Reznik, F. Gebhard and S. D. Baranovskii, *Release of carriers from traps enhanced by hopping*, Physical Review B **98**(15), 155207 (2018), doi:10.1103/PhysRevB.98.155207.

[66] H. F. Haneef, A. M. Zeidell and O. D. Jurchescu, *Charge carrier traps in organic semiconductors: A review on the underlying physics and impact on electronic devices*, Journal of Materials Chemistry C **8**(3), 759 (2020), doi:10.1039/c9tc05695e.

[67] J. E. Gentle, *Mathematical and statistical preliminaries*, In *Statistics and Computing*, pp. 5–79. Springer New York, doi:10.1007/978-0-387-98144-4_1 (2009).

[68] S. V. Melkonyan, *Non-Gaussian conductivity fluctuations in semiconductors*, Physica B: Condensed Matter **405**(1), 379 (2010), doi:10.1016/j.physb.2009.08.096.

[69] J. Ruseckas, R. Kazakevicius and B. Kaulakys, *Coupled nonlinear stochastic differential equations generating arbitrary distributed observable with 1/f noise*, Journal of Statistical Mechanics **2016**(4), 043209 (2016), doi:10.1088/1742-5468/2016/04/043209.

[70] N. Leibovich and E. Barkai, *Conditional $1/f^{\alpha}$ noise: From single molecules to macroscopic measurement*, Physical Review E **96**, 032132 (2017), doi:10.1103/PhysRevE.96.032132.

[71] https://github.com/akononovicius/flicker-trap-detrap-individual-charge.